GEOLOGICA BELGICA (2004) 7/1-2: 55-69

ALTERATION, MINERALISATION AND FLUID FLOW CHARACTERISTICS IN THE BIERGHES SILL, ANGLO-BRABANT FOLD BELT, BELGIUM

Stijn DEWAELE & Philippe MUCHEZ

(6 figures, 4 tables, 1 plate)

Fysico-chemische Geologie, K.U. Leuven, Celestijnenlaan 200C, B-3001 Leuven, Belgium.
E-mail: stijn.dewaele@geo.kuleuven.ac.be

ABSTRACT. In the Lower Palaeozoic of the Brabant Massif (Belgium) several polysulphide mineralisations associated with faults, have been identified. A multistage mineralised quartz-carbonate vein system occurs in the Bierghes sill. Macroscopic observations, geochemical and mineralogical investigations indicate a narrow alteration envelope around the veins, characterised by carbonitisation, sericitisation, chloritisation and silicification. The veins dominantly consist of dolomite and later generations of quartz. The opaque minerals are pyrite, galena and chalcopyrite. Vein development, alteration and the polysulphide mineralisation in the Bierghes sill can be considered contemporaneous with deformation and occurred after cleavage development. The mineralising fluids have a low-salinity H_2O-CO_2-X-NaCl-KCl composition, and a $\delta^{18}O$, $\delta^{13}C$ and $\delta^{34}S$ isotopic composition of respectively +5.5 to +7.5 ‰ V-SMOW, –11.8 to –10.5‰ V-PDB and – 2.8 ‰ to +1.8 ‰ CDT. The mineralisation at Bierghes is interpreted as a mesozonal orogenic mineralisation, which formed by the circulation of fluids with a metamorphic signature. The location of the Bierghes mineralisation in the same high strain zone as the mineralisation at the Marcq area, indicates an extensive circulation of metamorphic fluids along shear zones at the northern margin of a supposed granitoid basement block, during the late Silurian to early Devonian deformation of the Anglo-Brabant Fold belt.

KEYWORDS: Anglo-Brabant Fold belt, Bierghes sill, mesothermal vein system, fluid inclusions, stable isotopes, chlorite geothermometry

1. Introduction

Fluid flow in the deeper subsurface is often largely influenced by faults, which can act as highly permeable pathways for mineralising fluids. In an extensional tectonic regime, substantial quantities of fluids are expelled during normal faulting (Muir-Wood & King, 1993). In a region of compressional deformation, arrays of extension fractures develop by hydraulic fracturing adjacent to reverse faults prior to failure (Sibson, 1994). Failure of the reverse faults allows fluids from the overpressured reservoirs to migrate upwards. Typical examples of such fault-valve action are the mesozonal gold mineralisation hosted in steep reverse faults and brittle-ductile shear zones (Sibson *et al*., 1988, Sibson 1994; Cox *et al*., 1991; Robert *et al*., 1995; Groves *et al*. 1998; McCuaig &, Kerrich, 1998).

The study area is located at Bierghes, situated in the Senne valley (Fig. 1). The intrusive body found at this locality, can be classified as a dacitic metaporphyry (André, 1983). In the quarry in this sill (Fig. 1), new outcrops with a multistage mineralised quartz-carbonate vein system became exposed due to recent excavations (Figs 2A and B). In the Bierghes sill, several deformation features have been identified and described (Corin & Ronchesne, 1936a, b; Corin *et al*., 1963; Schippers, 1979; André & Deutsch, 1985; Debacker, 2001). According to Schippers (1979) and André & Deutsch (1985) the quartz-carbonate veins (Figs 2B to D) formed during Givetian strike-slip deformation.

The southern margin of the Lower Palaeozoic Anglo-Brabant Fold belt is characterised by a complex and particular deformation history due to the presence of an inferred rigid granitoid basement block at depth (Everaerts *et al*., 1996; Sintubin, 1999; Sintubin & Everaerts, 2002). Different faults, vein systems and associated polysulphide mineralisation have been identified at this margin of the fold belt (Fig. 1). The vein system in the Marcq area (Fig. 1) has been identified as a mesozonal orogenic mineralisation formed during the tectonometamorphic deformation of the Anglo-Brabant fold belt (Piessens *et al*., 2002). The migration of metamorphic fluids has been dated at 416 ± 3 Ma (Dewaele *et al*., 2002). However, the faults at the southern margin of the Anglo-Brabant Fold belt have been active during different geological time periods (Bergerat & Vandycke, 1994; Vandycke *et al*., 1991; Vandycke, 2002), even up to today (Oudenaarde earthquake 1938).

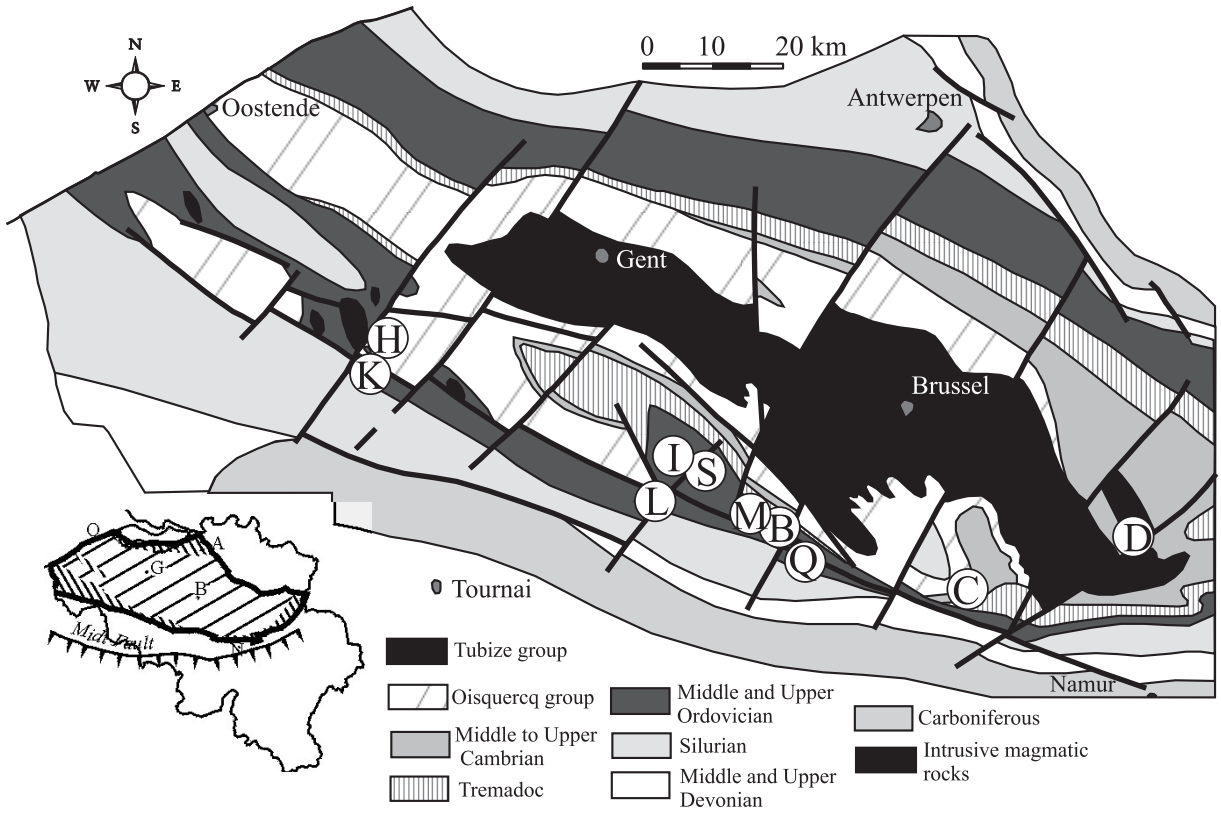

Fig. 1: Subcrop map of the Brabant Massif (after De Vos *et al*., 1993), with indication of the study area. B = Bierghes, C = Court St.-Etienne, D = Dongelberg, H = Hulste, I = Idegem, K = Kuurne, L = Lessines, M = Marcq area, S = Schendelbeke and Q = Quenast.

The aim of this study is to characterise and to determine the origin of the mineralising fluid in the Bierghes sill. Since this magmatic body falls in the high-strain zone north of the supposed granitoid crustal block at depth (Sintubin & Everaerts, 2002), the fluid characteristics are compared to those of the polysulphide mineralisation in the Marcq area. This allows us to obtain a more general view of fluid migration along the southern margin of the Anglo-Brabant Fold belt.

2. Geological setting

The Lower Palaeozoic rocks in central Belgium, northern France and the Netherlands form the southeastern part of the Anglo-Brabant Fold belt (Van Grootel *et al*., 1997; Verniers *et al*. 2002). This Caledonian slate belt is moulded around the Cadomian Midlands microcraton, forming the core of the East Avalonia microcontinent (Blundell *et al*., 1992).

This Anglo-Brabant Fold belt (Fig. 1) consists of folded, faulted and weakly metamorphosed rocks. Its sedimentary and tectonometamorphic evolution can be divided in three megasequences (Verniers *et al*., 2002), related to the palaeogeographic evolution of the East Avalonian microcontinent. During the first megasequence (Cambrian until early Ordovician), Avalonia is still connected to Gondwana. More specific, the Anglo-Brabant area has been identified as an extensional rift basin at the margin of Gondwana (e.g. Nance *et al*., 2002; Sintubin & Everaerts, 2002). During the Middle Ordovician, Avalonia disconnected from Gondwana and migrated northward as an isolated continental fragment (second megasequence). Finally, Avalonia encountered Baltica and collided with Laurentia during the Middle Silurian (Verniers *et al*., 2002). The oldest sediments in the Anglo-Brabant fold belt are of Early Cambrian age and occur in the central part of this fold belt (Fig. 1). Middle Cambrian to Silurian rocks flank this Cambrian core to the north and south. The Anglo-Brabant Fold belt in Belgium is characterised by a dominance of turbidity sediments. These sediments consist of claystones and siltstones, which were subjected to lower diagenetic up to greenschist metamorphic conditions (Van Grootel *et al*., 1997).

Several volcanic and intrusive rocks are distinguished along the southern margin of the Anglo-Brabant Fold belt (Fig. 1). The rocks have a dominantly dacitic composition, with some rhyolites and rare andesitic and basaltic rocks (Hertogen & Verhaeren, 1999; Verniers *et al*., 2002). The intrusive rocks of the Bierghes sill can be classified as dacitic. The rocks found at the Quenast plug have a similar composition, while the intrusive rocks of the Lessines sill are more andesitic (André, 1983). Based on composition and

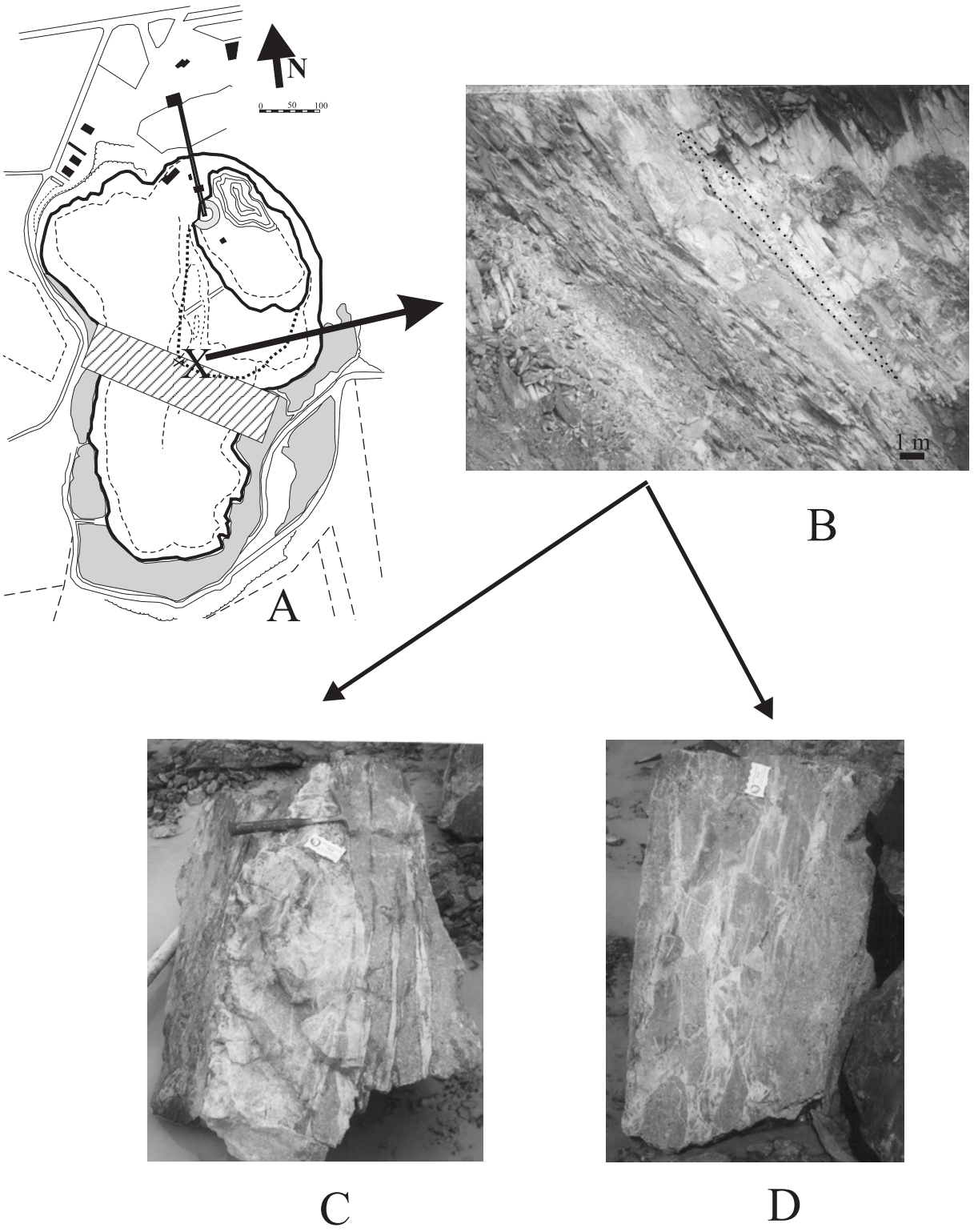

Fig. 2: A. Schematic plan of the quarry at Bierghes (after Schippers, 1979). Shaded area indicates zone with carbonate-quartz veins. Study area is indicated with X. B. Photograph of study area, dots indicate mineralised vein. C & D. Example of carbonate-quartz veins

distribution, the intrusive rocks are related to volcanic rocks, which are supposed to have formed as subaerial and submarine ignimbrites (Hertogen & Verhaeren, 1999). The magmatism has been related to a short-lived subduction of oceanic lithosphere from probably a small oceanic basin within the Avalonia microcontinent (Debacker, 2001; Verniers *et al.,* 2002) beneath the Avalonian microcontinent during Early Ashgill, i.e. the end of the second megasequence (André *et al*, 1986; Van Grootel *et al*., 1997; Verniers *et al.,* 2002).

Deformed Lower Palaeozoic basement metasediments are discordantly concealed by Givetian sediments, while the latest deformed sediments are of Ludlovian age (Debacker, 2001, Verniers *et al*., 2002). At present, there is only evidence for one major tectonometamorphic deformation of the Anglo-Brabant fold belt in Belgium, occurring during the Late Silurian to early Middle Devonian (André *et al*., 1981; Van Grootel *et al*., 1997; Debacker, 2001; Verniers *et al*., 2002; Dewaele *et al*., 2002). Since the accretion of Eastern Avalonia to Baltica occurred during the Late Ordovician to Early Silurian (Cocks *et al*., 1997; Verniers *et al*., 2002), the deformation in the Anglo-Brabant Fold belt can be considered as the result of a post-accretionary intracontinental accommodation within the East Avalonia microcontinent due to the closure of the Rheic Ocean (Pickering & Smith, 1995; Cocks *et al*., 1997; Rey *et al*., 1997). The Anglo-Brabant Fold belt in Belgium is recently considered as a compressional wedge system, where material is pushed out during the tectonometamorphic deformation phase (Sintubin & Everaerts, 2002). At the southwestern margin of this belt a low-density body is identified at depth, recently interpreted to be a Precambrian crustal block of granitoid composition (Everaerts *et al*., 1996; Sintubin & Everaerts, 2002). This fault-bounded basement block controlled the deformation and a NW-SE trending high-strain zone developed along its northeastern edge (Sintubin, 1999; Sintubin & Everaerts, 2002). The low-angle reverse shear zone, identified in the Marcq area (Fig. 1), can be considered as the result of this thrusting (Debacker, 1999).

The study area is the Bierghes sill (Figs 1 and 2). According to André (1983), this intrusion crystallised at the same time, from the same magma as the Quenast plug, which has been dated by U-Pb at 433 +/- 10 Ma (André & Deutsch, 1984). The Bierghes sill is however characterised by a widespread set of fracture/foliation planes with different orientation. Detailed observations in the quarry made it possible to distinguish a cleavage with an orientation of N20W41N and a fracture directed N60W50N (Fig. 3). The fracture planes seem to cut the foliation (Fig. 3). Fractures and foliation are better developed in the central part of the quarry, where also the dolomite-quartz veins are present (Corin *et al*., 1963; Schippers, 1979). These veins are clearly oriented parallel to the fracture planes (Fig. 2B). According to Legrand (1968), this zone forms part of the Oudenaarde-Bierghes fault zone, which has been identified to form part of the Nieuwpoort-Asquempont fault zone (De Vos *et al*. 1993; Sintubin, 1999; Debacker, 2001). André & Deutsch (1985) interpreted the veins as syn-tectonic; they formed during strike-slip faulting in the late Givetian (~373 ± 11 Ma).

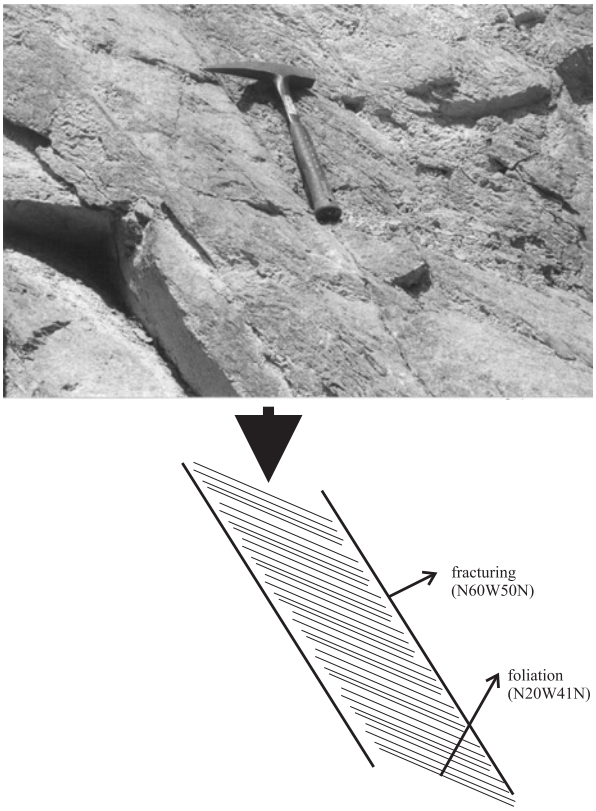

Fig. 3. Photograph and drawing of fractures and foliation

3. Methodology

Different samples have been taken from the quartz-carbonate vein system in the Bierghes sill for petrographic, mineralogical and geochemical investigation. The combination of different geochemical techniques allows to study the fluid-rock interaction. Fluid inclusion analysis has been carried out to identify fluid remnants trapped in mineral phases. Stable isotope composition was investigated to determine the origin of the fluids.

3.1 Mineral chemistry

Thin sections were prepared to determine the mineralogy of the vein minerals, the alteration zone and the host-rock. Examination of polished sections led to the identification of the ore minerals. The mineralogy of the fine-grained crystals (e.g. sericite, chlorite and other phyllosilicates) in the altered and unaltered rocks was determined by X-ray diffraction. The measurements were conducted on a Phillips PW3710 diffractometer with Cu-tube. The major element geochemistry of the host rock, and of the different alteration zones and vein types, has been measured by Atomic Absorption spectrometry (AAS).

Chlorite geothermometry was carried out on two polished thin sections with chlorite, present in two different stages of vein development. The Si, Al,

Fe, Mn, Mg, Ti content of the chlorites was measured with a Cameca France SX 50 electron microprobe using the standards fayalite (Si), sapphire (Al), hematite (Fe), olivine (Mg), rhodonite (Mn) and rutile (Ti). From the Al in the tetrahedral position and eventually the Fe/(Fe+Mg) ratio, the formation temperature of the chlorites can be calculated with the empirical models of Cathelineau (1988), Hillier & Velde (1991) and Jowett (1991). The thermodynamic model of Walshe (1986) uses the complete chemical composition of the chlorites to calculate their precipitation temperature at given pressure.

3.2 Fluid inclusion microthermometry

Doubly polished sections (300 μm thick) were prepared for the study of fluid inclusions in the gangue minerals. A detailed description of the sample preparation technique and of the measurement procedure has been given by Muchez *et al*. (1994). Microthermometric analyses of fluid inclusions were carried out on a Fluid Inc. adapted U.S.G.S. gas-flow heating-freezing system, mounted on an Olympus BX60 microscope. Reproducibility was within 0.2°C for the melting temperatures and < 3°C for the total homogenisation temperature (Th_{Tot}).

Since no Raman analysis have been carried out to determine the additional gas components, the maximum salinity and density of the fluid inclusions with an H_2O(-CO_2-(X))-NaCl-KCl composition, with X the additional gas components, has been estimated with the program Flincor of Brown (1989), using the Equation Of State (EOS) of Brown & Lamb (1989) for an H_2O-CO_2-NaCl system.

3.3 Stable isotope chemistry

The isotopic composition of the dolomite, present in the alteration zones and veins ($\delta^{18}O$ and $\delta^{13}C$), and of sulphides ($\delta^{34}S$) was measured to determine the origin of the mineralising fluids. The different dolomite generations and sulphides were selected based on their occurrence in the paragenetic sequence and sampled by diamond micro-drilling. Carbonate powders were reacted with 100% phosphoric acid (density > 1.9 g/cm^3, Wachter and Hayes, 1985) at 75°C in an online carbonate preparation line (Carbo-Kiel – single sample acid bath) connected to a Finnigan Mat 252 mass spectrometer. All values are reported in per mil relative to V-PDB. The oxygen isotopic composition of the dolomites was corrected using the fractionation factors given by Rosenbaum & Sheppard (1986). Reproducibility is better than 0.04‰. Oxygen and carbon stable isotopic analyses were carried out at the University of Erlangen, Germany. $\delta^{34}S$ analysis of sulphides were analysed by standard techniques at the SURRC centre in East Kilbride, Scotland. The SO_2 gas was liberated by combusting the sulphides with excess Cu_2O at 1075°C, in vacuo (Robinson and Kusakabe, 1975). Liberated gases were analysed on a VG Isotech SIRA II mass spectrometer. Reproducibility is better than 0.2‰ (1σ). Data are reported in $\delta^{34}S$ notation as per mil (‰) variations from the Canyon Diablo Troilite (CDT) standard.

4. Petrography and mineral paragenesis

The primary -unaltered- magmatic rocks dominantly consist of feldspar (especially albite), amphibole, pyroxene and quartz. Ilmenite, apatite, zircon and magnetite are present as accessory minerals. Epidote and chlorite are the most important secondary minerals (e.g. André, 1983). The original magmatic texture has however significantly been altered by relatively low-temperature secondary processes. Hydrothermal activity linked to the injection of dacitic magmas within water-saturated Ordovician sediments (André & Deutsch, 1986), metamorphism associated with the Early Devonian deformation phase (André *et al*, 1981) and fluid flow causing a Late Givetian to Late Devonian Sr resetting (André & Deutsch, 1985) could have resulted in an intense sericitic alteration of feldspars, epidotisation, chloritisation and saussuritisation.

Since the orientation of the mineralised veins is identical to that of the fractures, their development is thought to be related to this fracturing. The isolated veins seem to form lenses, which have a thickness up to a metre. The veins are found in a NW-SE oriented zone (N60W50N) transecting the quarry (Fig. 2A). The quartz-dolomite veins are associated with an alteration characterised by dolomitisation, silicification and sericitisation. A polysulphide mineralisation occurs in the veins.

A detailed scheme of the mineral paragenesis of the multistage mineralised quartz-carbonate vein system is presented in Fig. 4, indicating five main stages in its evolution. In an initial step, bands of green-coloured altered rocks are formed (=stage 1). This alteration stage consists of dolomite, quartz, muscovite and chlorite (Plate 1A). This stage is followed by the formation of red-coloured altered rocks, consisting of dolomite, quartz, muscovite and hematite (=stage 2). The latter mineral is responsible for the red colouring of the rocks (Plate 1B). The alteration is followed by vein generation 1 (=stage 3), which dominantly consists of dolomite (Plate 1C). Traces of muscovite are present, but chlorite is absent. Some quartz occurs as a late vein-filling phase. This vein generation also contains pyrite, chalcopyrite and galena (Plate 1D). The pyrites are often characterised by a cataclastic deformation. The next vein generation 2 consists of dolomite and quartz (=stage 4). The last generation 3 formed perpendicular to the former vein generation and only contains quartz (=stage 5).

The alteration stages are characterised by carbonitisation, chloritisation, silicification and sericitisation compared to the host rocks. This is

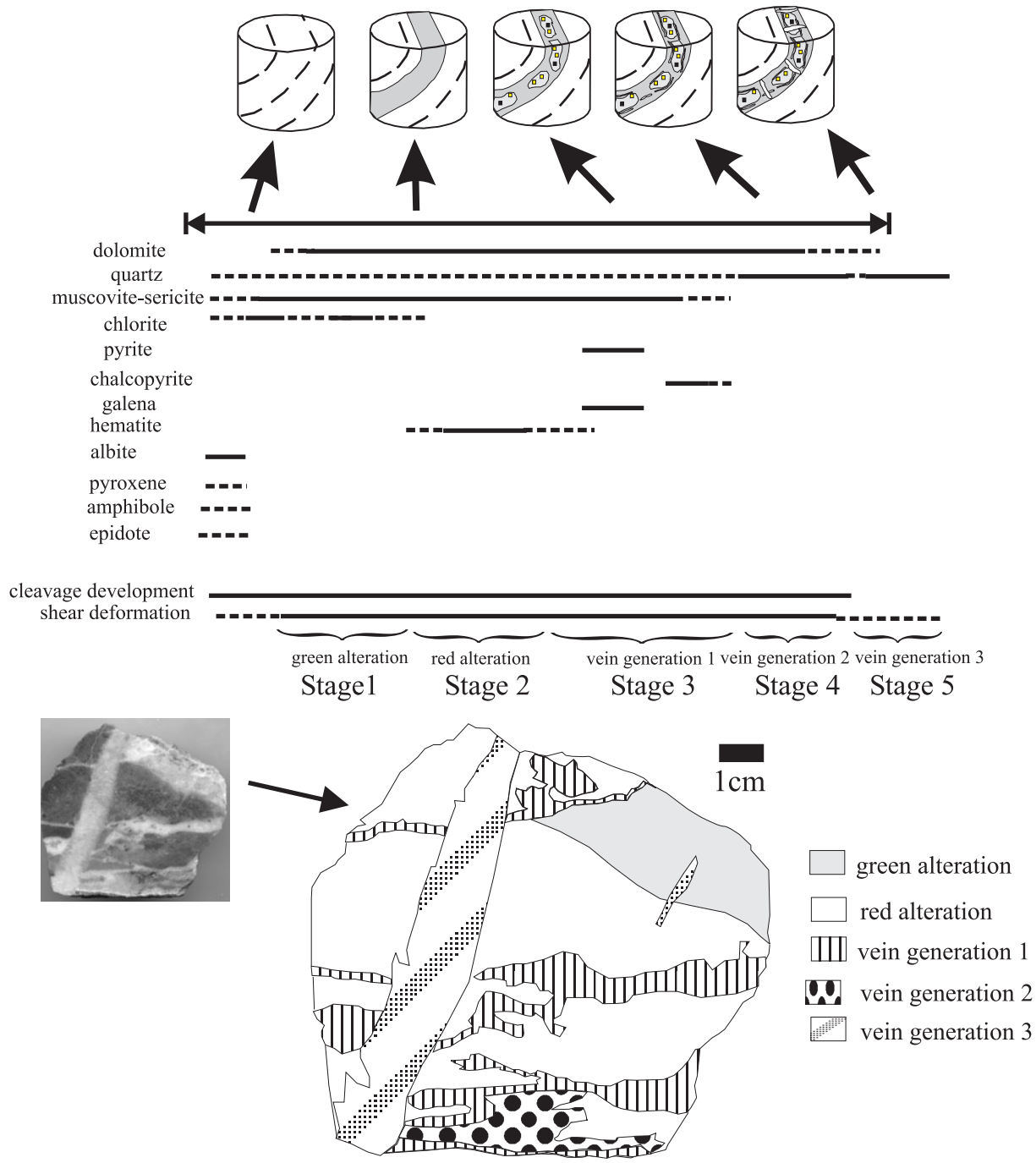

Fig. 4. Paragenesis of the vein system in the Bierghes sill with schematic illustration of the formation of some characteristic vein types. See text for explanation of the different stages

illustrated by the geochemical analysis (Table 1), which shows a higher concentration of MnO, K_2O and CaO in the green-coloured alteration, compared to the host rocks. The Al_2O_3, MgO and TiO_2 content remains similar, while there is a decrease of Na_2O, Fe_2O_3 and SiO_2. Additionaly, the red-coloured alteration is characterised by the highest amount of Fe_2O_3, MnO, MgO and CaO; but the lowest concentration of SiO_2, TiO_2, Al_2O_3, K_2O and Na_2O. While sericite is omnipresent in the alteration stages and in the first vein generation, chlorite can only be identified in the green-coloured alteration. This observation has been confirmed by X-ray diffraction. Some remains of strongly altered feldspars can still be identified in the green-coloured alteration.

5. Microthermometry

Doubly-polished sections have been investigated from vein generation 1, 2 and 3. The fluid inclusions in vein generation 1 were studied in dolomite, while fluid inclusions in vein generation 2 and 3 were measured in quartz. Due to the complex, progressive deformation history of the earliest generations of veins,

Sample	SiO2	TiO2	Al2O3	Fe2O3	MnO	MgO	CaO	Na2O	K20	LOI	Total
33m from vein	62.67	0.71	14.53	6.93	0.03	5.27	0.52	1.90	2.91	4.05	98.97
22m from vein	64.32	0.72	14.33	6.09	0.03	3.52	1.36	3.06	2.74	3.64	99.36
11m from vein	62.66	0.71	14.68	5.85	0.08	4.10	1.34	2.36	3.02	4.60	98.92
11m from vein	63.10	0.70	14.13	5.72	0.02	4.01	1.19	2.38	2.99	5.00	98.71
wallrock adjacent vein	64.47	0.60	13.40	5.29	0.02	5.65	0.93	0.84	3.25	5.27	99.20
green-coloured alteration	50.55	0.67	14.42	5.14	0.17	5.38	6.34	0.25	4.82	12.14	99.59
red-coloured alteration	29.75	0.07	3.48	7.44	1.37	9.37	16.26	0.01	1.22	31.30	99.68
red-coloured alteration	28.02	0.05	3.68	9.25	1.35	9.35	15.90	0.01	1.20	31.30	99.53

Table 1. Major element geochemistry of the host rock, and of the different alteration zones at Bierghes.

it was impossible to determine the chronology of fluid inclusions in vein generations 1 and 2. Only in vein generation 3, it was possible to distinguish between primary and secondary inclusions.

The fluid inclusions in vein generation 1 are two-phase (L + V) aqueous-gaseous inclusions at room temperature (Plate 1E). Some isolated three phase inclusions have been found. The melting temperature of CO_2 (Tm_{CO2}) is only measurable in the largest inclusions, since the formation of clathrate consumed the majority of CO_2. Tm_{CO2} is -57.5°C (Fig. 5A). Since this temperature is below –56.6 °C, it indicates the presence of one or several gasses, CH_4, N_2, H_2S, …, in addition to CO_2. In a few inclusions the eutectic melting temperature of the aqueous phase could be measured and is around –22°C, indicative for the presence of KCl in addition to NaCl (Shepherd *et al.*, 1985). The ice melting temperatures (Tm_{Ice}) vary between – 3.8°C and –5.3°C (Fig. 5B). Clathrate dissociation temperatures (Tm_{Clath}) occur between 7.6°C and 8.4°C (Fig. 5C). The homogenisation of the CO_2 (Th_{Tot}) can be measured in few inclusions and varies between 24.8 and 28.0 °C. Decrepitation occurs at a temperature of 240°C, and total homogenisation temperatures vary between 237 °C and 363°C (Fig. 5D). The two-phase aqueous-gaseous inclusions have an H_2O-CO_2-(X)-NaCl-KCl composition, with X the additional gas components. The calculated maximum salinity and density for all measured inclusions respectively vary between 6.0 and 8.2 eq. wt% NaCl, and 0.67 and 0.88 g/cm^3.

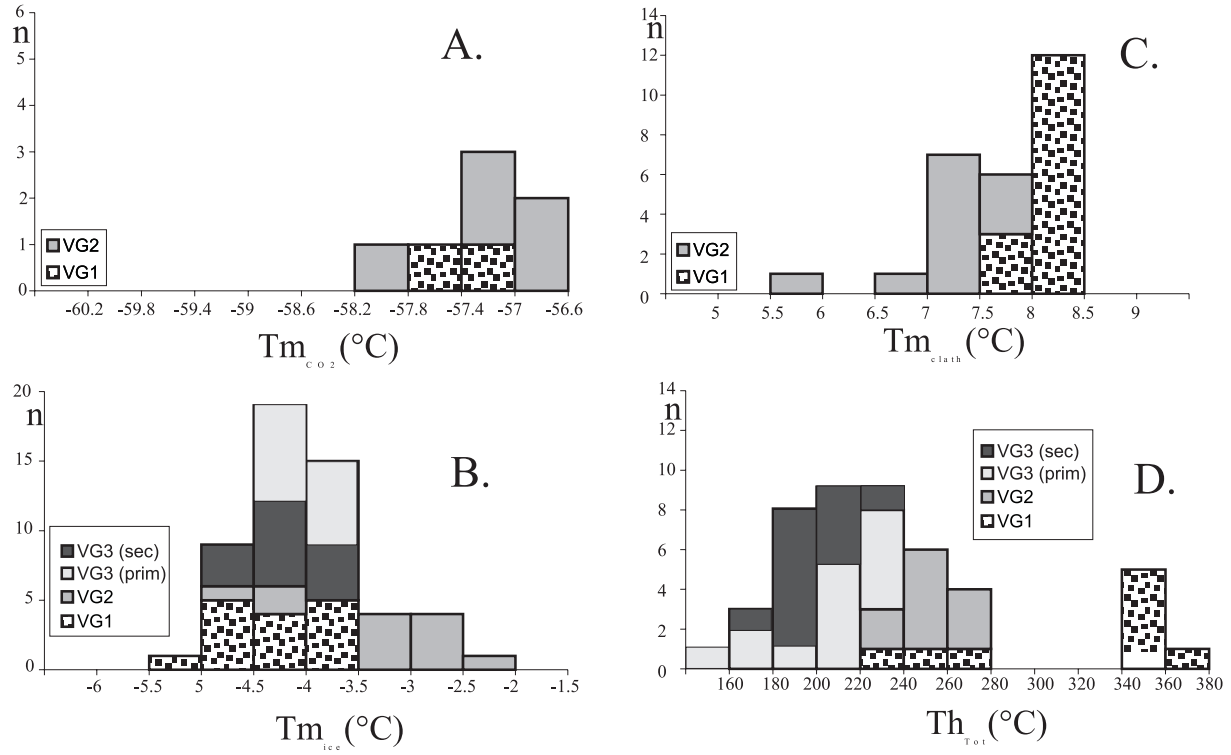

Fig. 5. Microthermometric data of aqueous-gaseous and aqueous fluid inclusions in dolomite or quartz associated with the Bierghes vein system. VG1 = vein generation 1, VG2 = vein generation 2, VG3(prim) = primary inclusions in vein generation 3 and VG3(sec) = secondary inclusions in vein generation 3.
Melting temperature of CO_2 (Tm_{CO2}); Melting temperature of ice (Tm_{Ice}); Melting temperature of clathrate (Tm_{Clath}); Total homogenisation temperature (Th_{Tot})

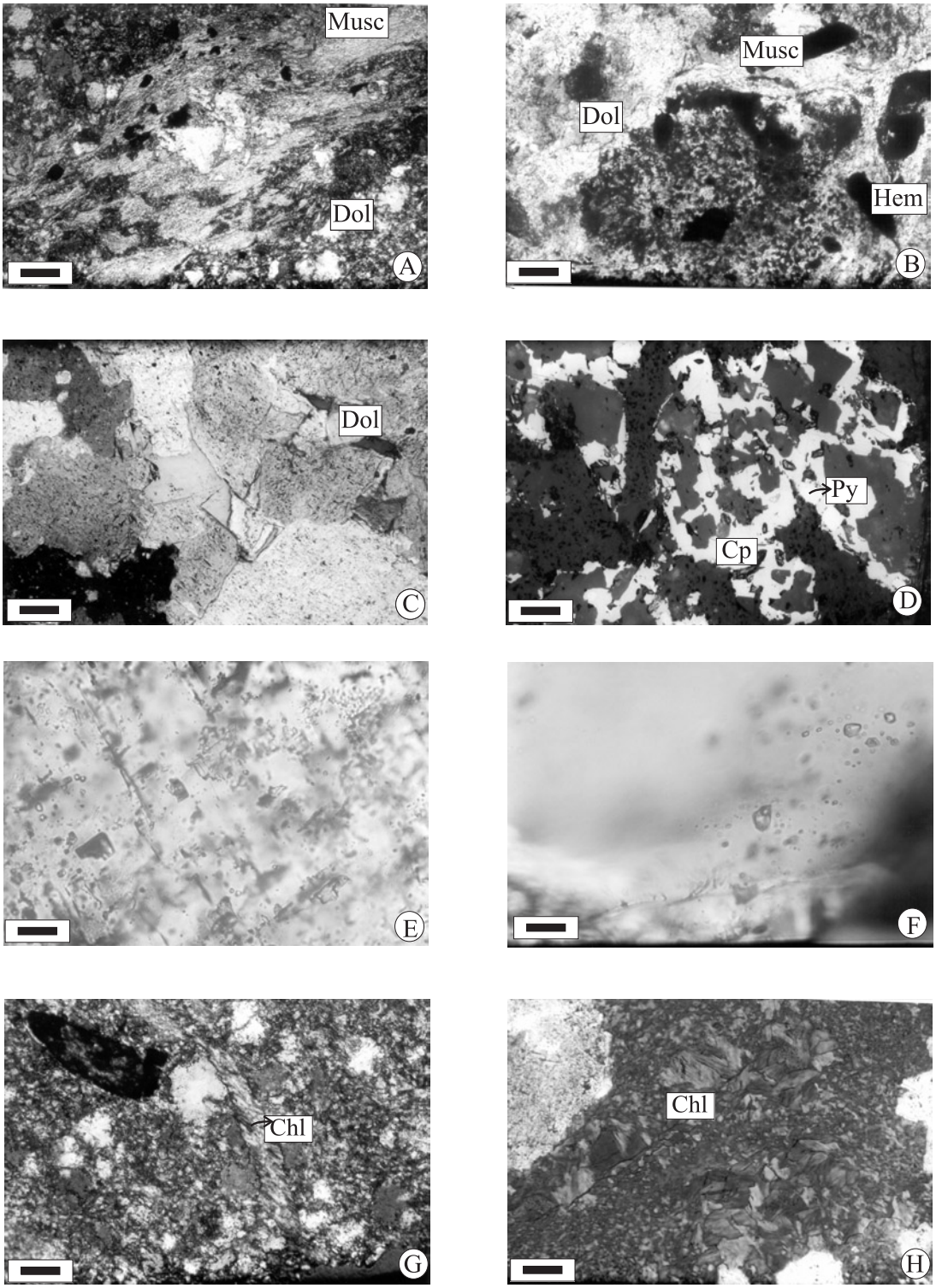

PLATE 1

A. Photograph of green-coloured alteration. Note the preferred orientation of the muscovite fibers. Muscovite (Musc); dolomite (Dol). Crossed nicols. Scale bar is 135 μm.

B. Photomicrograph of red-coloured alteration. Note presence of muscovite (Musc); hematite (Hem); dolomite (Dol). Crossed nicols. Scale bar is 65 μm.

C. Photomicrograph of vein generation 1, dominantly consisting of dolomite. Crossed nicols. Scale bar is 65 μm.

D. Photomicrograph showing detail of sulphide mineralisation at Bierghes. Cp =chalcopyrite, Py = pyrite. Scale bar is 65 μm.

E. Detail of a trail showing two-phase aqueous fluid inclusions in dolomite. Scale bar is 35 μm.

F. Detail of the trail showing two-phase aqueous-gaseous fluid inclusions in vein generation 3. Scale bar is 35 μm.

G. Photomicrograph of chlorite type 1, occurring in the green-coloured alteration zone. Crossed nicols. Scale bar is 65 μm.

H. Photomicrograph of chlorite type 2, at the contact of the green-coloured and red-coloured alteration zones. Crossed nicols. Scale bar is 65 μm.

A	Analysis	SiO_2	TiO_2	Al_2O_3	FeO	MnO	MgO	H_2O
Green alteration	1	25.31	0.087	18.59	20.56	0.164	17.52	17.77
	2	26.00	0.050	19.18	20.99	bd	18.17	15.60
	3	26.44	0.058	19.20	20.92	0.097	18.10	15.18
	4	26.13	0.045	19.20	20.99	0.134	18.10	15.40
	5	25.91	bd	19.20	21.12	0.115	17.80	15.84
	6	25.91	bd	19.22	21.00	0.125	18.18	15.53
Border green-red alteration	1	28.87	0.063	19.83	12.51	bd	24.64	14.10
	2	28.18	0.052	19.95	12.73	0.096	24.55	14.45
	3	27.62	bd	20.26	13.57	bd	24.08	14.44
	4	38.23	0.315	23.91	8.32	bd	14.02	15.21
	5	27.99	bd	19.94	13.11	0.093	24.09	14.74
	6	28.12	bd	19.65	13.13	bd	24.40	14.66

B	Analysis	Si	Ti	Al(tetr)	Al(oct)	Fe	Mn	Mg
Green alteration	1	2.79	0.0075	1.21	1.21	1.89	0.014	2.88
	2	2.79	0.0040	1.21	1.21	1.88	bd	2.90
	3	2.81	0.0048	1.18	1.23	1.86	0.008	2.87
	4	2.79	0.0032	1.20	1.22	1.87	0.012	2.88
	5	2.78	bd	1.21	1.23	1.90	0.010	2.85
	6	2.78	bd	1.21	1.21	1.88	0.011	2.90
Border green-red alteration	1	2.88	0.0450	1.11	1.23	1.04	bd	3.37
	2	2.83	0.0380	1.16	1.21	1.07	0.077	3.68
	3	2.79	bd	1.20	1.21	1.14	bd	3.63
	4	3.65	0.0220	0.35	2.34	0.66	bd	1.99
	5	2.83	bd	1.16	1.21	1.11	0.007	3.63
	6	2.84	bd	1.15	1.19	1.11	bd	3.68

Table 2A. Geochemical composition (weight%) of the chlorites found in the green alteration and the border of the green-red alteration. **B**. Calculated composition of chlorites by unit cell.

The fluid inclusions of vein generation 2 are two-phase (L + V) aqueous-gaseous inclusions at room temperature in quartz. Also, some isolated three phase inclusions have been found. Tm_{CO2} was measurable in a limited number of inclusions and varies between –56.6 °C and –57.9 °C (Fig. 5A). Three temperatures are below –56.6 °C, indicating the presence of an extra gas phase in addition to CO_2. The eutectic melting temperature of the aqueous phase is ~ –22°C, indicative for the presence of KCl in addition to NaCl in the aqueous phase (Shepherd *et al*., 1985). Tm_{Ice} varies between –2.5° and –5.5°C (Fig. 5B). Tm_{Clath} values are between 5.8°C and 7.3°C (Fig. 5C). Th_{Tot} of the inclusions occurs between 235 °C and 265 °C (Fig. 5D). Like the inclusions in the first vein generation, the fluid inclusions in the second vein generation have an H_2O-CO_2-(X)-NaCl-KCl composition. The calculated maximum salinity and density for all measured inclusions respectively vary between 4.5 and 8.5 eq. wt% NaCl, and 0.83 and 0.88 g/cm^3.

The fluid inclusions of vein generation 3 are two-phase (L + V) aqueous-gaseous inclusions at room temperature (Plate 1F). In this vein generation, a chronology of different orientations of fluids was observable. However, only a small decrease in homogenisation temperatures can be observed in the secondary fluid inclusions (Fig. 5D). No traces of CO_2 or another gas phase have been found. The temperature of eutectic melting of the aqueous phase could be measured and lies around ~ –21.0°C, indicative for the H_2O-NaCl system. Tm_{Ice} varies between –3.6° and –4.4°C (Fig. 5B). Th_{Tot} values are between 158 °C and 235 °C, with an average of 200 °C (Fig. 5D). The salinity and density has been calculated for all measured inclusions and the values vary respectively between 5.7 and 6.9 eq. wt% NaCl, and between 0.88 and 0.95 g/cm^3.

6. Chlorite geochemistry

Two types of chlorite have been recognised at Bierghes. The first type occurs in the green-coloured alteration, while the second chlorite occurs at the contact between the green and the red-coloured alteration. The first type of chlorite has a blue-greenish anisotropy colour (Plate 1G), while the second generation has a distinct light green colour (Plate 1H). According to the chlorite classification diagram of Hey (1954), the first chlorite has a composition between ripidolite and pycnochlorite, while the second type of chlorite has a composition dominantly corresponding to clinochlore (Table 2 and Figure 6). This means that the latter type of chlorite is Mg-richer. The composition of the chlorite, found in the green-coloured alteration of the Bierghes vein system, has a different composition from the chlorites found associated with veins in the Marcq area (Dewaele *et al*. 2001), the Bolland borehole (Zhang *et al*., 1997) and the Stavelot Massif (Schroyen, 2000; Schroyen & Muchez, 2000). The chlorites in these latter areas have a ripidolite to daphnite composition (Fig. 6).

From the Al in the tetrahedral position and eventually the Fe/(Fe+Mg) ratio, the formation temperature of the chlorites has been calculated with the empirical models of Cathelineau (1988), Hillier &

Velde (1991) and Jowett (1991) and with the thermodynamic model of Walshe (1986). The different chlorite geothermometers show no distinct variation between the average values of the two types of chlorite (Table 3). The geothermometer of Cathelineau (1988) and Jowett (1991) show a similar temperature (~320°C), while Hillier & Velde (1991) results in a lower temperature of 265° C. The geothermometer of Walshe indicates a temperature of 280°C for 100 MPa and of 300°C for 200 MPa (Table 3).

The different chemical composition of the chlorites present in the Bierghes vein system, compared to the veins in the Marcq area, Bolland borehole and the Stavelot Massif likely reflect a different equilibration temperature (Dewaele *et al*. 2001, Zhang *et al*., 1997, Schroyen, 2000; Schroyen & Muchez, 2000; Dewaele *et al*. 2001). However, buffering of the chemical composition of the fluids by the surrounding rocks can not be excluded. Chlorite geothermometry should always be supported by additional temperature indicators (De Caritat *et al*., 1993).

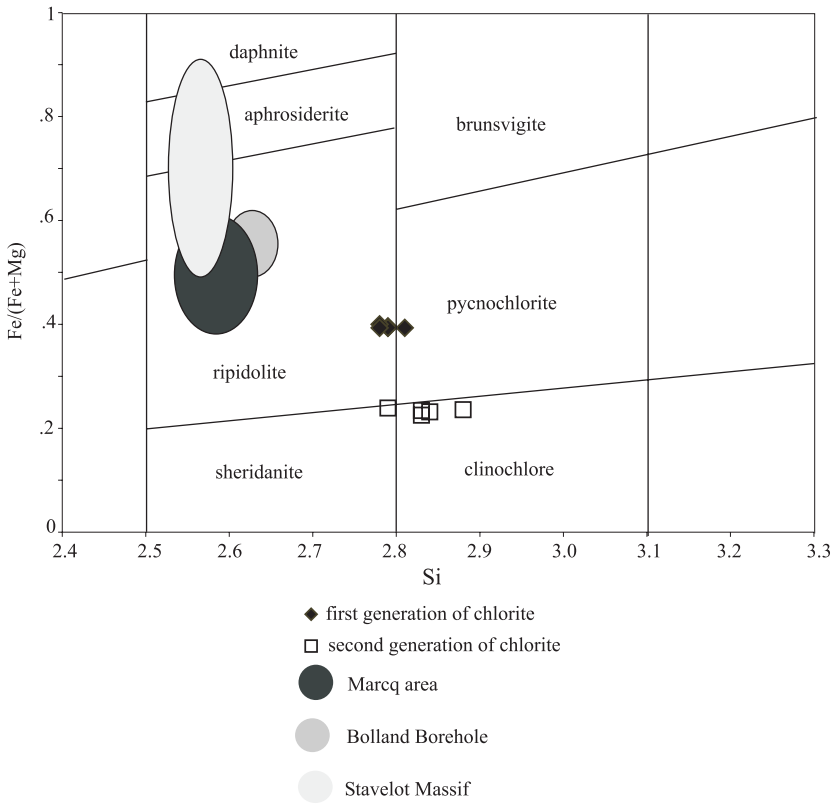

Fig. 6. Geochemical classification of the chlorite found in the Bierghes sill, after Hey (1954). First generation of chlorite is indicated by black diamonds, while second generation by squares. Additional data from the Marcq area (Dewaele *et al*., 2001), Bolland borehole (Zhang *et al*., 1997) and Stavelot Massif (Schroyen, 2000) is given.

Model	green alteration min T (∞C)	green alteration max T (∞C)	green alteration **Average T (∞C)**	border green-red alteration min T (∞C)	border green-red alteration max T (∞C)	border green-red alteration **Average T (∞C)**
Cathelineau	318	328	**322**	295	324	**317**
Hillier & Velde	264	279	**270**	229	274	**262**
Jowett	319	329	**323**	292	321	**316**
Walshe: 0.1 MPa	248	265	**254**	231	280	**258**
100 MPa	267	288	**278**	255	288	**280**

Table 3. Geothermometry of the two chlorite types in alteration zones at Bierghes, calculated with the empirical models of Cathelineau (1988), Hillier & Velde (1991) and Jowett (1991) and the thermodynamic model of Walshe (1986). Minimum and maximum calculated values are given, the average value is printed bold.

7. Stable isotope analyses

Ten dolomite samples have been selected for stable isotope analyses ($\delta^{18}O$, $\delta^{13}C$). Samples have been taken from the two alteration zones and from the different vein generations. The isotopic composition of the dolomites and of five sulphides ($\delta^{34}S$) was measured to determine the origin of the mineralising fluids. The $\delta^{18}O$ values and $\delta^{13}C$ values vary respectively between +13 ‰ and +14.5 ‰ V-SMOW and between –12.4 ‰ and –14.3 ‰ V-PDB (Table 4). Pyrite has $\delta^{34}S$ values between – 2.8 ‰ and +2.9 ‰ CDT, while the investigated galena sample has a value of –5.6 ‰ CDT (Table 4).

By using the formation temperature of the dolomite and the sulphides, it is possible to calculate the original isotopic composition of the mineralising fluid. The formation temperature of the sulphides has been estimated by using coexisting sulphide pairs that precipitated at equilibrium conditions (Ohmoto & Rye, 1979). Coexisting pyrite (–2.8 ‰ CDT) and galena (–5.6 ‰ CDT) have a $\Delta_{py\text{-}gn}$ of 2.8, indicating a precipitation temperature of 300-350°C. This calculated temperature based on isotopic fractionation between coexisting sulphide minerals is in good agreement with the temperature obtained by fluid inclusion microthermometry. It should be noticed that if the precipitation temperature changes with 50°C, the $\delta^{18}O$ and $\delta^{13}C$ values of the fluids change by respectively ~ 2 ‰ and ~ 0.8 ‰. $\delta^{34}S$ values are less effected by temperature fractionation (Ohmoto & Goldhaber, 1997). The calculated oxygen ($\delta^{18}O$) and carbon ($\delta^{13}C$) isotopic

	$\delta^{13}C_{V\text{-}PDB}$ (‰)	$\delta^{18}O_{V\text{-}SMOW}$ (‰)	$\delta^{34}S_{CDT}$ (‰)
green alteration	-12.7	13.1	
green alteration	-12.4	13.3	
red alteration	-13.3	13.4	
green alteration	-13.8	13.1	
red alteration	-14.2	13.1	
vein generation 1	-12.3	13.6	
vein generation 1	-12.3	13.6	
vein generation 2	-12.5	13.2	
vein generation 2-3	-13.8	13.2	
vein generation 2-4	-12.6	14.5	
pyrite			-2.8
pyrite			0.7
pyrite			2.9
pyrite			-0.3
pyrite			1.8
galena			-5.6

Table 4. Results of stable isotope analyses of dolomite ($\delta^{18}O$, $\delta^{13}C$), and sulphides ($\delta^{34}S$) in veins at Bierghes vein system. V-SMOW: Vienna-standard mean ocean water, V-PDB: Vienna Peedee Belemnite, CDT: Canyon Diablo meteorite troilite.

composition of the ambient fluid fall respectively, between +5.5 ‰ and +7.5 ‰ V-SMOW and between –10.5 ‰ and –11.8 ‰ V-PDB. The sulphur ($\delta^{34}S$) isotopic composition varies between – 2.8 ‰ and +2.9 ‰ CDT.

8. Discussion

8.1 Structural setting

In the multistage mineralised quartz-dolomite vein system at Bierghes, the occurrence of the sulphides is restricted to the vein generation 1. The fracture-parallel orientation of the mineralised veins and the deformation of the sulphides demonstrate that the mineralisation took place during a progressive deformation in which the fracture planes were reactivated as fluid pathways. Based on Rb-Sr radiometric dating, André & Deutsch (1985) interpreted the veins to be syn-tectonic during Late Givetian (373 ± 11 Ma) shear strike-slip faulting. The authors interpreted this age as an ^{87}Sr resetting of the intrusive rocks by hydrothermal circulation along the shear zone at temperatures below 250°C (André & Deutsch, 1985). Resetting of Rb-Sr whole rock ages has been proven by the formation of secondary hydrated minerals by water-rock interaction from Rb-rich minerals (biotite, K-feldspar) and acid ash-flow tuffs in rocks affected by low-grade metamorphism (Evans, 1991; Evans *et al.*, 1995). Since the first vein generation in the quartz-dolomite vein system has homogenisation temperatures up to 350°C and temperatures of 250°C are only found in vein generation 2 and 3, the age obtained by André & Deutsch (1985) is considered as a minimum age of the mineralisation in the Bierghes sill. Since mineralised fractures are cutting the cleavage planes, vein generation post-dates cleavage development. The structural setting and timing of the veins at Bierghes can be compared with the polysulphide mineralisation in the Marcq area. In the Marcq area, the mineralisation, alteration and deformation occurred largely during the same progressive deformation event, slightly post-dating the development of the cleavage fabric. The alteration, which formed contemporaneous with the mineralisation (Piessens *et al.*, 2002), has been dated to have occurred 416 ± 3 Ma ago, during the main deformation phase of the Anglo-Brabant Fold belt in Belgium (Dewaele *et al.*, 2002).

The alteration around the veins at Bierghes, developed along thin NE-dipping zones, parallel to the fracture planes. Such a well-defined pattern reflects a strong tectonic control on the migration of the fluids. Geochemical and XRD analysis showed an alteration pattern, characterised by carbonitisation, sericitisation, silicification and chloritisation features. Mineralisation with this kind of alteration pattern in magmatic rocks is often recognised in mesozonal orogenic mineralisation. It is caused by the alteration of mostly mafic and ultramafic rocks by a CO_2-rich fluid (Ash & Arksey, 1989; Kishida & Kerrich, 1987; Leitch *et al.*, 1991). Carbonate minerals which replace these rocks form by hydrolysis of iron, magnesium, calcium and manganese silicates to carbonates in which the wall rocks provide the bivalent metal cations (Kerrich, 1989). At Bierghes, André & Deutsch (1985) and Schippers (1979) interpreted the carbonates as the results of the dynamometamorphic breakdown of epidote. Mesozonal orogenic deposits occur worldwide, from the Archean to the Tertiairy (Goldfarb *et al.*, 2001). Typical Phanerozoic orogenic deposits are associated with convergent plate margins, in close proximity to major translithospheric structures or transpressional-transtensional shear zones (Bierlein & Crowe, 2000). Mesozonal orogenic deposits are almost entirely structurally controlled, and often formed at or above the brittle-ductile transition in greenschist terranes.

8.2 Fluid temperatures

The hydrothermal system of the multistage mineralised quartz-carbonate vein system found at Bierghes is characterised by three groups of fluids. CO_2-rich fluids have been identified in vein generation 1 and 2. In vein generation 1 the homogenisation temperature falls between 237°C and 363°C, while in vein generation 2 T_{hTot} varies between 235°C and 265°C. Detailed observation of the T_{hTot} distribution plot indicates two clusters for vein generation 1 (Fig. 5D). The cluster between 341 and 363°C could correspond to the unaltered fluids of vein generation 1 and forms a minimum range of trapping temperatures for vein generation 1. The cluster of lower temperatures between 237° and 277°C could correspond to fluids of vein generation 1, reset by

the fluids in vein generation 2 (T_{hTot} between 235° and 265°C). Fluids from vein generation 2 could also partly have reset other minerals, e.g. chlorite, which could explain the lower temperatures obtained by the chlorite geothermometers.

The fluids associated with vein generation 3 can be considered as a late, relatively low temperature fluid (minimum temperature between 158° and 235°C), with a different composition as the fluids from vein generation 1 and 2.

8.3 Fluid composition and origin

Fluids with an H_2O-CO_2-(X)-NaCl-KCl composition have also been identified in the vein system in the Marcq area (Dewaele *et al*., 2001; Piessens *et al*., 2002), which has been identified as a typical mesothermal orogenic fluid formed by the circulation of metamorphic fluids (Piessens *et al*., 2002). This fluid composition is characteristic for the Phanerozoic polysulphide and gold mineralisation in the Caledonides of the British Isles (Shepherd *et al*, 1991; Bottrel *et al*., 1988; Duller *et al*., 1997; Ixer *et al*., 1997; Mason, 1997; Steed & Morris, 1997; Lowry *et al*. 1997; Wilkinson *et al*. 1999). However, the mineralisation in these areas are often associated with granitic intrusions. The main emplacement of the Bierghes sill is restricted to the Ashgillian (Late Ordovician). It preceeds the deformation event in the Anglo-Brabant Fold belt, occurring during the Late Silurian to Early Devonian, by at least 30 Ma (André *et al*, 1981; Van Grootel *et al*. 1997; Debacker, 2001; Verniers *et al*. 2002; Dewaele *et al*., 2002). Magmatic fluids can therefore be excluded as the dominant source or transport medium for the mineralisation. The alternative explanation, involving mainly metamorphic fluids, is in complete agreement with the tectonometamorphic framework.

The metamorphic origin of the fluid is supported by the isotopic investigations. The $\delta^{18}O$ composition of the dolomitising fluids at Bierghes (between +5.5 ‰ and +7.5 ‰ V-SMOW), is similar to the isotopic composition of the fluid causing the mineralisation in the Marcq area (+3 to +8 ‰ V-SMOW), which has been identified as a metamorphic fluid (Piessens *et al*., 2002). The $\delta^{13}C$ values of the dolomite are negative, between –10.5 ‰ and –11.8 ‰ VPDB, which can be explained by the diagenesis/metamorphism of organic material-rich sediments (Ohmoto & Goldhaber, 1994). The $\delta^{34}S$ range between –2.8 ‰ and +2.9 ‰ CDT, falls in the range of I-type magmatic rocks (-5 to 5 ‰ CDT). However, the isotopic signature of sulphides is strongly depending on the $\delta^{34}S$ composition of sulphides and sulphates in the country rocks (Ohmoto & Goldhaber, 1997; Ohmoto, 1986). This indicates that the $\delta^{34}S$ values of the Bierghes sulphides certainly do not exclude a metamorphic origin. Based on the geotectonic setting, the similarity with the Marcq area and the lack of clear evidence for a magmatic origin, the mineralising fluid at Bierghes is interpreted to have a metamorphic origin. It should be stated that only fluids from vein generation 1 and 2 are likely to have a metamorphic origin. Fluids from vein generation 3 can be anything, notably surface waters (e.g. marine waters), that infiltrated at depth.

This study has demonstrated a spatial and temporal relationship between alteration, polysulphide mineralisation and deformation in the Anglo-Brabant fold belt in Belgium. The vein system in the Bierghes sill is the second location identified, in addition to the Marcq area, where a migration of metamorphic fluids, accompanied by progressive deformation along a high-strain zone, is proposed. Both areas are located in the same fault zone, located at the northeastern edge of a low-density body, identified at depth (Sintubin, 1999; Sintubin & Everaerts, 2002). This granitoid basement block controlled the deformation (Sintubin, 1999; Sintubin & Everaerts, 2002) and associated faults acted as conduits for the release of metamorphic fluids during the Lower Palaeozoic deformation of the Anglo-Brabant Fold belt in Belgium.

9. Conclusion

The alteration and polysulphide mineralisation in the Lower Palaeozoic magmatic rocks in the Bierghes sill are spatially associated with NE dipping fracture planes. The zone of alteration and mineralisation comprises several small lenses, up to one metre thick. The total thickness of the mineralised zone is 50 metres. Mineralisation and alteration occurred during progressive deformation, but after cleavage development.

The mineralising fluids have an H_2O-CO_2-(X)-NaCl-KCl composition. The $\delta^{18}O$, $\delta^{13}C$ and $\delta^{34}S$ isotopic composition of the fluids is respectively between +5.5 ‰ to 7.5 ‰V-SMOW, –10.5 to – 11.5 ‰ V-SMOW and – 2.8 ‰ to +2.9 ‰ CDT. These fluids caused the precipitation of the sulphide minerals and the carbonitisation, sericitisation, silicification and chloritisation of the host rock.

The vein system in the Bierghes sill has been identified as a mesozonal orogenic mineralisation. The mineralising fluids most likely had a metamorphic origin, based on the geotectonic and geochemical characteristics. The similarity between the vein system in the Bierghes sill and the polysulphide mineralisation in the Marcq area, reflects a related origin.

The occurrence of the veins at Bierghes in the same geotectonic context as those in the Marcq area, indicates an important migration of metamorphic fluids in the high-strain zone at the northern margin of the supposed granitoid basement block, during the Lower Palaeozoic deformation of the Anglo-Brabant Fold belt, Belgium.

Acknowledgements
Funding was provided by the Fund of Scientific Research of Flanders (F.W.O.-Vlaanderen, Belgium) project G.0274.99. Ir Jacques Wautier is sincerely thanked for the electron microprobe analysis at the "Centre d'analyse par microsonde pour les Sciences de la Terre" at Louvain-la-Neuve. Herman Nijs carefully prepared thin sections and the doubly polished wafers. Thanks to Ir. Jean Fourdin of C.U.P., for the authorisation to visit and study the quarry at Bierghes. Prof. Dr. M. Sintubin and Dr. T. Debacker are thanked for the discussion on the field. Dr. M. Joachimski is thanked for the $\delta^{18}O$ and $\delta^{13}C$ analysis of the dolomites at the University of Erlangen (Germany) and Dr. A. Boyce for the $\delta^{34}S$ analysis of the sulphides at the SURRC centre in East Kilbride (Scotland). We like to thank Prof. Dr. L. André and Prof. Dr. J.L.R. Touret for carefully reviewing the manuscript and their constructive suggestions.

10. References.

ANDRE, L., 1983. Origine et évolution des roches éruptives du Massif du Brabant (Belgique). Unpublished PhD thesis, Université Libre de Bruxelles.

ANDRE, L. & DEUTSCH, S., 1984. Les porphyres de Quenast et de Lessines : Géochronologie, géochimie isotopique et contribution au problème de l'age du socle précambrien du Massif du Brabant (Belgique). *Bulletin de la Société Belge de Géologie*, 93, 375-384.

ANDRE, L. & DEUTSCH, S., 1985. Very low-grade metamorphic Sr isotopic resetting of magmatic rocks and minerals : Evidence for a late Givetian strike-slip division of the Brabant Massif (Belgium). *Journal of the Geological Society of London*, 142, 911-923.

ANDRE, L. & DEUTSCH, S., 1986. Magmatic $^{87}Sr/^{86}Sr$ relicts in hydrothermally altered quartz diorites (Brabant Massif, Belgium) and the role of epidote as a Sr filter. *Contributions to Mineralogy and Petrology*, 92, 104-112.

ANDRE, L., DEUTSCH, S. & MICHOT, J., 1981. Données géochronologiques concernant le développement tectono-métamorphique du segment Calédonien Brabançon. *Annales de la Société Géologique de Belgique*, 104, 241-253.

ANDRE, L., HERTOGEN, J. & DEUTSCH, S., 1986. Ordovician-Silurian magmatic provinces in Belgium and the Caledonian orogeny in middle Europe. *Geology*, 14, 879-882.

ASH, C.H. & ARKSEY, R.L., 1989. The Listwanite- lode gold association in British Columbia. British Columbia Geological Survey Branch. Geological Fieldwork 1989, Paper 1990-1.

BERGERAT, F. & VANDYCKE, S. 1994. Palaeostress analysis and geodynamic implations of Cretaceous-Tertiairy faulting in Kent and the Boulonnais. *Journal of the Geological Society of London*, 151, 439-448.

BIERLEIN, F.P. & CROWE, D.E., 2000. Phanerozoic orogenic lode gold deposits. *Reviews in Economic Geology*, 13, 103-139.

BLUNDELL, D.J., FREEMAN, R. & MUELLER, S, 1992. A Continent Revealed. The European Geotraverse. Cambridge University Press, Cambridge.

BOTTRELL, S.H., SHEPHERD, T.J., YARDLEY, B.W.D. & DUBESSY, J., 1988. A fluid inclusion model for the genesis of the ores of the Dolgellau Gold Belt, North Wales. *Journal of the Geological Society of London*, 145, 139-145.

BROWN, E.B., 1989. FLINCOR: a microscopic program for the reduction and investigation of fluid inclusions data. *American Mineralogist*, 74, 1390-1393.

BROWN, E.B. & LAMB, W.M., 1989. P-V-T properties of fluids in the system H_2O-CO_2-NaCl: new graphical presentations and implications for fluid inclusion studies. *Geochimica et Cosmochimica Acta,* 53, 1209-1221.

CATHELINEAU, M., 1988. Cation site occupancy in chlorites and illites as a function of temperature. *Clay Minerals,* 23, 471-485.

COCKS, L., McKERROW, W., VAN STAAL, C., 1997. The margins of Avalonia. *Geological Magazine*, 134, 627-636.

CORIN, F. & RONCHESNE, P., 1936a. Contribution à l'étude du gisement des roches éruptives de Bierghes (Brabant). *Annales de la Société Géologique de Belgique*, 59, 61-66.

CORIN, F. & RONCHESNE, P., 1936b. Une mylonite dans le porphyre de Bierghes (Brabant). *Annales de la Société Géologique de Belgique,* 59, 66-68.

CORIN, F., FRANCART, J.-P. & VAN TASSEL, R., 1963. Etude géologiques de la carrière de Bierghes. Les filons de carbonates. *Bulletin de la société belge de Géologie, de Paléontologie et d'Hydrologie*, 72, 150-177.

COX, S.F., WALL, V.J., ETHERIDGE, M.A. & POTTER, T.F., 1991. Deformational and metamorphic processes in the formation of mesothermal vein-hosted gold deposits - examples from the Lachlan Fold Belt in central Victoria, Australia. *Ore Geology Reviews*, 6, 391-423.

DEBACKER, T.N., 1999. Folds trending at various angles to the transport direction in the Marcq area, Brabant Massif. *Geologica Belgica*, 2, 159-172.

DEBACKER, T.N., 2001. Palaeozoic deformation of the Brabant Massif within eastern Avalonia: how, when and why? Unpublished PhD thesis, Ghent University.

DE CARITAT, P., HUTCHEON, I. & WALSHE, J.L., 1993. Chlorite geothermometry: a review. *Clays and Clay Minerals*, 41, 219-239.

DE VOS, W., VERNIERS, J., HERBOSCH, A. & VANGUESTAINE, M., 1993. A new geological map of the Brabant Massif, Belgium. *Geological Magazine*, 130, 605-611.

DEWAELE, S., MUCHEZ, PH., PIESSENS, K., VANDEGINSTE, V. & BURKE, E.A.J., 2001. P-T-X variation along a polysulphide mineralised low-angle shear zone in the Lower Palaeozoic Anglo-Brabant fold

belt (Belgium). *In* Piestrzynski et al. (Eds) -Mineral deposits at the beginning of the 21st century, 727-730.

DEWAELE, S., BOVEN, A. & MUCHEZ, PH., 2002. $^{40}Ar/^{39}Ar$ dating of a mesothermal orogenic low-angle reverse shear zone in the Lower Palaeozoic of the Anglo-Brabant fold belt, Belgium. *Transactions of Institution of Mining and Metallurgy. (Section B: Applied Earth Sciences),* 111, 214-219.

DULLER, P.R., GALLAGHER, M.J., HALL, A.J. & RUSSELL, M.J., 1997. Glendinning deposit - an example of turbidite-hosted arsenic-antimony-gold mineralization in the Southern Uplands, Scotland. *Transactions of Institution of Mining and Metallurgy. (Section B: Applied Earth Sciences*), 106, 119-134.

EVANS, J.A., 1991. Resetting of Rb-Sr whole-rock ages during Acadian low-grade metamorphism in North Wales. *Journal of the Geological Society of London*, 148, 703-710.

EVANS, J.A., MILLAR, I.L. & NOBLE, S.R. 1995. Hydratation during uplift is recorded by reset Rb-Sr whole-rock ages. *Journal of the Geological Society of London*, 152, 209-212.

EVERAERTS, M., POITEVIN, C., DE VOS, W. & STERPIN, M., 1996. Integrated geophysical/geological modelling of the western Brabant Massif and structural implications. *Bulletin de la Société Belge de Géologie*, 105, 41-59.

GOLDFARB, R.J., GROVES, D.I. & GARDOLL, S., 2001. Orogenic gold and geologic time: a global synthesis. *Ore Geology Reviews*, 18, 1-75.

GROVES D.I., GOLDFARB, RJ, GEBRE-MARIAM, M., HAGEMANN, S.G. & ROBERT, F., 1998. Orogenic gold deposits: A proposed classification in the context of their crustal distribution and relationship to other gold deposit types. *Ore Geology Reviews*, 13, 7-27.

HERTOGEN, J. & VERHAEREN, M., 1999. Studie van het magmatisme in het Massief van Brabant. Unpublished report ANRE. VLA96-3.5.4, K.U.Leuven (Belgium), 50pp.

HEY, M.H., 1954. A new review of the chlorites. *Mineralogical Magazine*, 30, 277-292.

HILLIER, S. & VELDE, B. ,1991. Octahedral occupancy and the chemical composition of diagenetic (low-temperature) chlorites. *Clay Minerals*, 26, 149-168.

IXER, R.A.F., PATTRICK, R.A.D. & STANLEY, C.J., 1997. Geology, mineralogy and genesis of gold mineralizations at the Calliachar-Urlar Burn, Scotland. *Transactions of Institution of Mining and Metallurgy. (Section B: Applied Earth Sciences),* 106, 99-108.

JOWETT, E.C., 1991. Fitting iron and magnesium into the hydrothermal chlorite geothermometer. Abstracts of the GAC/MAC/SEG Joint Annual Meeting (Toronto, May 27-29,1991), 16, A62.

KERRICH, R., 1989. Geochemical evidence on the source of fluids and solutes for shear zone hosted mesothermal Au Deposits. *In* Bursnal, J.T. (Ed) Mineralization in shear zones, *Geological Association of Canada, Short Course Notes*, Volume 6, pages 129-197.

KISHIDA, A., KERRICH, R., 1987. Hydrothermal alteration zoning and gold concentration at the Kerr-Addison Archean Lode gold deposit, Kirkland Land, Ontario. *Economic Geology*, 82, 649-690.

LEGRAND, R., 1968. Le Massif du Brabant. *Mémoires pour servir à l'Explication des cartes Géologiques et Minières de la Belgique*, Mémoire 9, 1-148.

LEITCH, C.H.B., GODWIN, C.I., BROWN, T.H. & TAYLOR, B.E., 1991. Geochemistry of mineralzing fluids in the Bralorne-Pioneer Mesothermal gold vein deposit, British Columbia, Canada. *Economic Geology*, 86, 318-353.

LOWRY, D., BOYCE, A.J., FALLICK, A.E. & STEPHENS, W.E., 1997. Sources of sulphur, metals and fluids in granitoid-related mineralization of the Southern Uplands, Scotland. *Transactions of Institution of Mining and Metallurgy. (Section B: Applied Earth Sciences),* 106, 157-168.

MASON, J.S., 1997. Regional polyphase and polymetallic vein mineralization in the Caledonides of the Central Wales Orefield. *Transactions of Institution of Mining and Metallurgy. (Section B: Applied Earth Sciences),* 106, 135-143.

McCUAIG, T.C. & KERRICH, R., 1998. P-T-t-deformation-fluid characteristics of lode gold deposits: evidence from alteration systematics. *Ore Geology Reviews*, 12, 381-453.

MUCHEZ, PH., MARSHALL, J.D., TOURET, J.L.R. & VIAENE, W.A., 1994. Origin and migration of palaeofluids in the Upper Viséan of the Campine Basin, northern Belgium. *Sedimentology*, 41, 133-145.

MUIR-WOOD, R. & KING, G., 1993. Hydrological signatures of earthquake strain. *Journal of Geophysical Research*, 98, 22035-22068.

NANCE, R.D., MURPHY, J.B. & KEPPIE, J.D., 2002. A Cordilleran model for the evolution of Avalonia. *Tectonophysics*, 352, 11-31.

OHMOTO, H., 1986. Stable isotope geochemistry of ore deposits. *In Valley, J.W., Taylor, H.P. & O'Neil, J.R.* (Eds.) - Stable isotopes in high temperature geological processes. *Reviews in Mineralogy*, 16, 419-559.

OHMOTO, H. & RYE, R.O., 1979. Isotopes of sulfur and carbon. *In* Barnes, H.L. (Ed.) - Geochemistry of hydrothermal ore deposits. John Wiley & Sons, New York, 509-567.

OHMOTO, H. & GOLDHABER, M.B., 1997. Sulphur and carbon isotopes. *In* Barnes, H.L. (Ed.) - Geochemistry of hydrothermal ore deposits. John Wiley & Sons, New York, 517-600.

PICKERING, K.T. & SMITH, A.G., 1995. Arcs and backarc basins in the Early Paleozoic Iapetus Ocean. *The Island Arc,* 4, 1-67.

PIESSENS, K., MUCHEZ, PH., DEWAELE, S., BOYCE, A., DE VOS, W., SINTUBIN, M., DEBACKER, T., BURKE, E.A.J. & VIAENE, W., 2002. Fluid flow, alteration, and polysulphide

mineralisation associated with a low-angle reverse shear zone in the Lower Palaeozoic of the Anglo-Brabant fold belt, Belgium. *Tectonophysics*, 348, 73-92.

REY, P., BURG, J.-P. & CASEY, M., 1997. The Scandinavian Caledonides and their relationship to the Variscan belt. *In* Burg, J.-P. & Ford, M. (Eds.) - Orogeny Through Time. *Geological Society of London, Special Publication*, 121 ,179-200.

ROBERT, F., BOULLIER, A.-M. & FIRDAOUS, K., 1995. Gold-quartz veins in metamorphic terranes and their bearing on the role of fluids in faulting. *Journal of Geophysical Research*, 100, 12861-12879.

ROBINSON, B.W. & KUSAKABE, M., 1975. Quantitative preparation of SO_2 for $^{34}S/^{32}S$ analysis from sulfides by combustion with cuprous oxide. *Analytical Chemistry*, 47, 1179-1181.

ROSENBAUM, J. & SHEPPARD, S.M., 1986. An isotopic study of siderites, dolomites and ankerites at high temperatures. *Geochimica and Cosmochimica Acta*, 50, 1147-1150.

SCHIPPERS, T. 1979. Etude structurale du Massif de Bierghes. Unpublished Licence thesis, Université Libre de Bruxelles.

SCHROYEN, K., 2000. Caledonische en Varistische fluïda en de metamorfe evolutie van het Stavelot-Vennmassief. Unpublished PhD thesis, K.U.Leuven.

SCHROYEN, K. & MUCHEZ, PH., 2000. Evolution of metamorphic fluids at the Variscan fold-and-thrust belt in eastern Belgium. *Sedimentary Geology*, 131, 163-180.

SHEPHERD, T.J., RANKIN, A.H. & ALDERTON, D.H.M., 1985. A practical guide to fluid inclusions studies. Blackie, London.

SHEPHERD, T.J., BOTTRELL, S.H. & MILLER, M.F., 1991. Fluid inclusion volatiles as an exploration guide to balck shale-hosted gold deposits, Dolgellau gold belt, North Wales, UK. *Journal of Geochemical Exploration*, 42, 1991, 5-24.

SIBSON, R., 1994. Crustal stress, faulting and fluid flow. *In* PARNELL, J. (Ed.) - Geofluids: Origin, migration and evolution of fluids in sedimentary basins. *Geological Society of London, Special Publication*, 78, 69-84.

SIBSON, R.H., ROBERT, F. & POULSEN, K.H., 1988. High-angle reverse faults, fluid pressure cycling and mesothermal gold-quartz deposits. *Geology,* 16, 551-555.

SINTUBIN, M., 1999. Arcuate fold and cleavage patterns in the southeastern part of the Anglo-Brabant Fold belt (Belgium): tectonic implications. *Tectonophysics*, 309, 81-97.

SINTUBIN, M. & EVERAERTS, M., 2002. A compressional wedge model for the Lower Palaeozoic Anglo-Brabant Belt (Belgium) based on potential field data. *In* Winchester, J.A., Pharaoh, T.C. & Verniers, J. (Eds.) -Palaeozoic amalgamation of Central Europe, *Geological Society of London, Special Publications*,201, 327-343.

STEED, G.M. & MORRIS, J.H., 1997. Isotopic evidence for the origins of a Caledonian gold-arsenopyrite-pyrite deposit at Clontibret, Ireland. *Transactions of Institution of Mining and Metallurgy (Secion B: Applied Earth Sciences),* 106, 109-118.

VANDYCKE, S., 2002. Palaeostress records in Cretaceous formations in NW Europe: extensional and strike-slip events in relationships with Cretaceous-Tertiairy inversion tectonics. *Tectophysics*, 357, 119-136.

VANDYCKE, S., BERGERAT, F. & DUPUIS, CH., 1991. Meso-Cenozoic faulting and inferred palaeostresses in the Mons Basin, Belgium. *Tectonophysics*, 192, 261-271.

VAN GROOTEL, G., VERNIERS, J., GEERKENS, B., LADURON, J., VERHAEREN, M., HERTOGEN, J. & DE VOS, W., 1997. Timing of magmatism, foreland basin development, metamorphism and inversion in the Anglo-Brabant fold belt. *Geological Magazine*, 134, 607-616.

VERNIERS, J., PHARAOH, T., ANDRE, L., DEBACKER, T.N., DE VOS, W., EVERAERTS, M., HERBOSCH, A., SAMUELSSON, J., SINTUBIN, M. & VECOLI, M., 2002. The Cambrian to mid Devonian basin development and deformation history of eastern Avalonia, east of the Midlands Microcraton: new data and a review. *In* Winchester, J.A., Pharaoh, T.C. & Verniers, J. (Eds.) -Palaeozoic amalgamation of Central Europe, *Geological Society of London, Special Publications*, 201, 47-93.

WACHTER, E. & HAYES, J.M., 1985. Exchange of oxygen isotopes in carbon-dioxide – phosphoric acid systems. *Chemical Geology*, 52, 365-374.

WALSHE, J.L., 1986. A six-components chlorite solid solution model and the conditions of chlorite formation in hydrothermal and geothermal systems. *Economic Geology*, 81, 681-703.

WILKINSON, J.J., BOYCE, A.J., EARLS, G. & FALLICK, T., 1999. Gold remobilisation by low-temperature brines: evidence from the Curraghinalt gold deposit, Northern Ireland. *Economic Geology*, 94, 289-296.

ZHANG, Y., MUCHEZ, PH. & HEIN, U.F., 1997. Chlorite geothermometry and temperature conditions at the Variscan thrust front in eastern Belgium. *Geologie en mijnbouw*, 76, 267-270.

Manuscript received 4.06.2003 ; accepted for publication 19.09.2003.